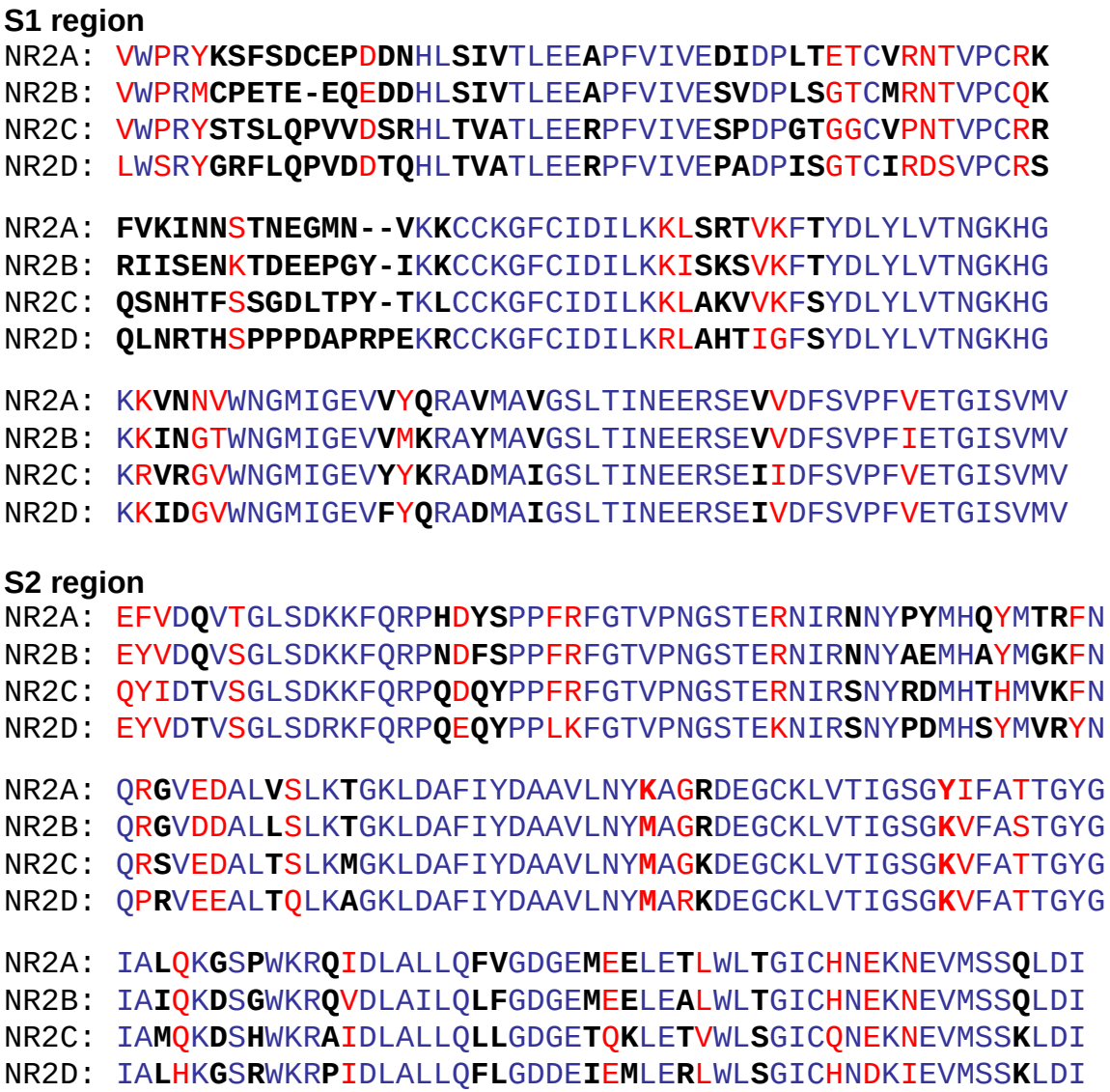

Supplemental Figure 1. Sequence alignments for S1 and S2 regions in NR2A, NR2B, NR2C and NR2D NMDAR subunits. Residues shown in blue are common to all four NMDAR subunits. Residues shown in red are common to three subunits, while those shown in bold black are either different in each of the four subunits or are common to only two subunits. The two locations in the S2 region where residues are conserved in NR2B, NR2C and NR2D NMDAR subunits but are different in the NR2A NMDAR subunit and result in a change in charge at such locations are shown in bold red. These are amino acids Lys719 (NR2A), Met713 (NR2B), Met717 (NR2C) and Met740 (NR2D) and Tyr735 (NR2A), Lys729 (NR2B), Lys733 (NR2C) and Lys756 (NR2D).

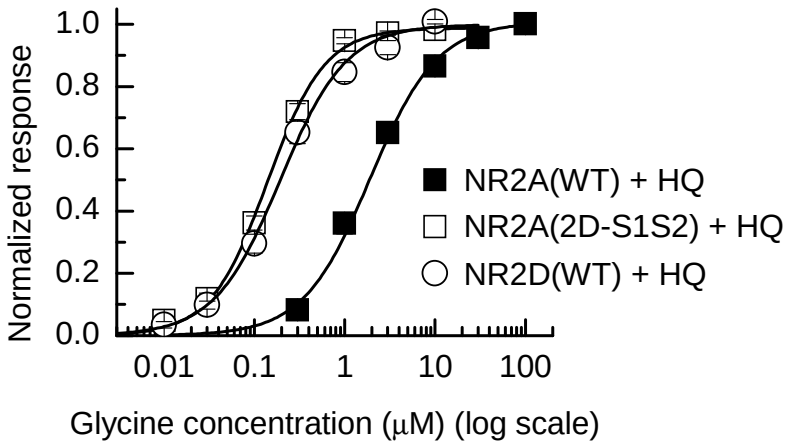

Supplemental Figure 2. Glycine concentration-response data for wild-type NR2A, NR2D and NR2A(2D-S1S2) NMDARs when homoquinolinate is used as the NR2 binding site agonist. The use of homoquinolinate (rather than glutamate) as the NR2 agonist does not alter the potency of glycine. EC_{50} values for glycine acting at each of these NMDAR combinations are given in the text. The mean Hill slopes and mean maximal currents recorded were for NR2A(WT): 1.17 ± 0.07, 3.5 ± 0.4 μA; NR2D(WT): 1.19 ± 0.06, 0.4 ± 0.06 μA and NR2A(2D-S1S2): 1.37 ± 0.06, 1.4 ± 0.7 μA.

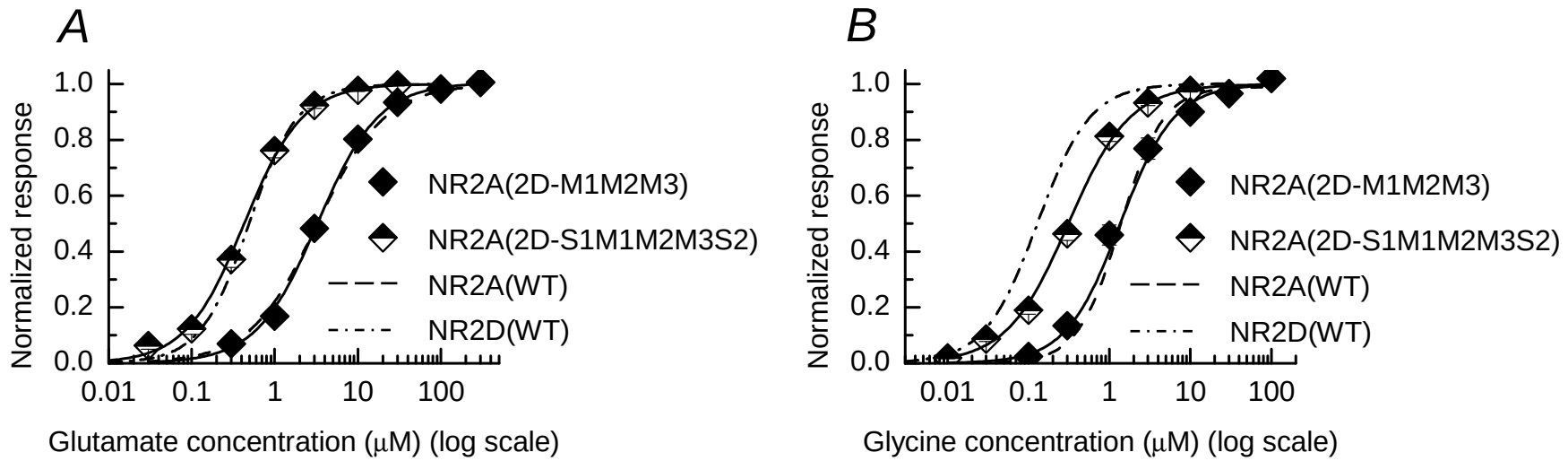

Supplemental Figure 3. Concentration-response curves for chimeric NMDARs where membrane associated domains and their intracellular linkers from NR2A have been replaced with those found in NR2D subunits. *A*, mean glutamate concentration-response curves for NR2A(2D-M1M2M3) and NR2A(2D-S1M1M2M3S2) constructs. Inclusion of the M1, M2 and M3 domains from the NR2D subunit in NR2A subunits does not alter glutamate potency compared to NR2A(WT)-containing NMDARs. When S1 and S2 regions are also included a shift to a NR2D-like potency is observed. For comparison, the dashed lines show the comparable curves for NR2A(WT)- and NR2D(WT)-containing NMDARs (from Erreger *et al.* 2007). For glutamate concentration-response curves, mean Hill slopes and mean maximal currents recorded were for NR2A(2DM1M2M3): 1.18 ± 0.04, 2.0 ± 0.1 μA and NR2A(2D-S1M1M2M3S2): 1.23 ± 0.05, 1.1 ± 0.2 μA. *B*, mean glycine concentration-response curves for NR2A(2D-M1M2M3) and NR2A(2D-S1M1M2M3S2) constructs. Inclusion of the M1, M2 and M3 domains from the NR2D subunit in NR2A subunits does not alter glycine potency compared to NR2A(WT)-containing NMDARs. When S1 and S2 regions are also included a shift to a more NR2D-like potency is observed. For comparison, the dashed lines show the comparable curves for NR2A(WT)- and NR2D(WT)-containing NMDARs. For glycine concentration-response curves, mean Hill slopes and mean maximal currents recorded were for NR2A(2D-M1M2M3): 1.30 ± 0.06, 1.4 ± 0.2 μA and NR2A(2D-S1M1M2M3S2): 1.14 ± 0.04, 0.5 ± 0.05 μA.

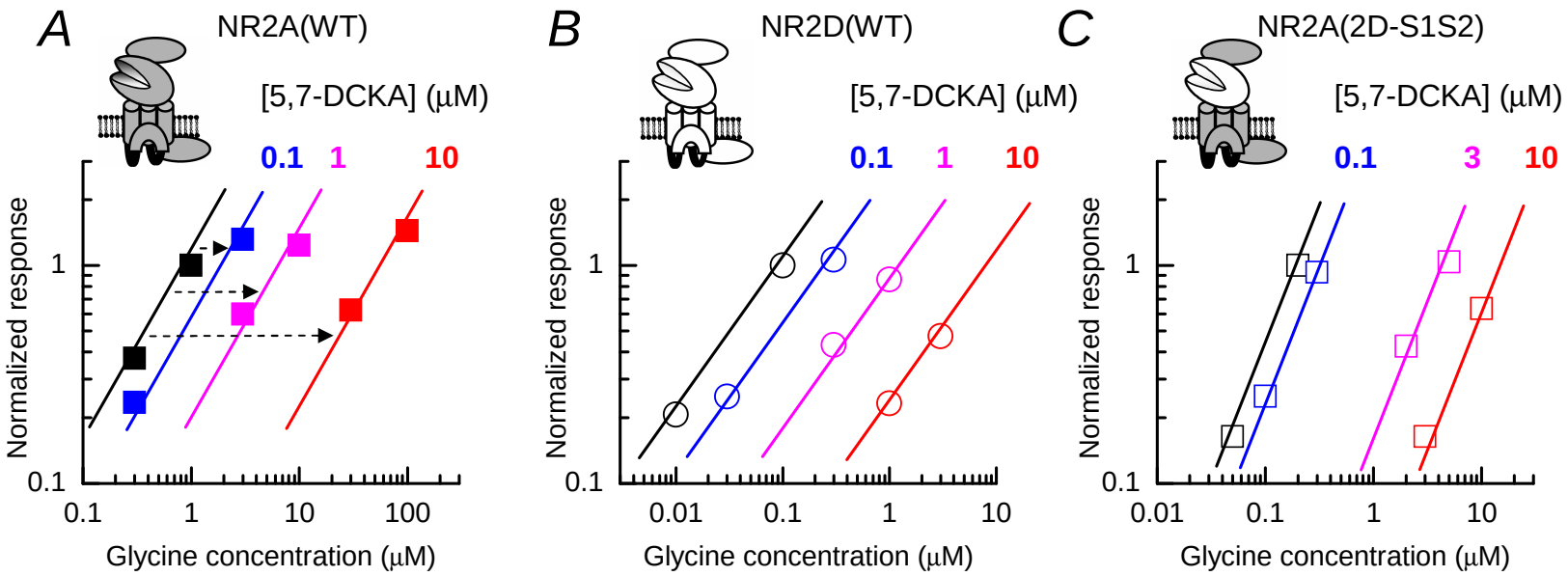

Supplemental Figure 4. Example two-point concentration response curves used to determine dose-ratios. *A*, partial, low concentration glycine-response curves for NR1/NR2A NMDAR-mediated currents generated in the absence or presence of increasing concentrations of 5,7-DCKA. *B*, as in *A*, but for glycine-evoked currents mediated by NR1/NR2D NMDARs. *C*, as in *A*, but for glycine-evoked currents mediated by NR1/NR2A(2D-S1S2) NMDARs. The concentrations of 5,7-DCKA used are indicated above each concentration-response curve (0.1 μM, 1 μM, 3 μM or 10 μM). In each case 5,7-DCKA results in a parallel shift to the right of the two-point concentration-response curve from which dose-ratios can be estimated (as indicated by the dashed arrows in *A*). Overall the mean dose-ratios (which are shown in Fig. 6*C-E*) were for NR1/NR2A NMDARs: 2.28 ± 0.3 (0.1 μM), 12.1 ± 3.1 (1 μM) and 137 ± 40 (10 μM); for NR1/NR2D NMDARs: 2.63 ± 0.3 (0.1 μM), 15.9 ± 3.4 (1 μM) and 115 ± 41 (10 μM); and for NR1/NR2A(2D-S1S2) NMDARs 2.28 ± 0.4 (0.1 μM), 37.4 ± 13.3 (3 μM) and 133 ± 42 (10 μM).

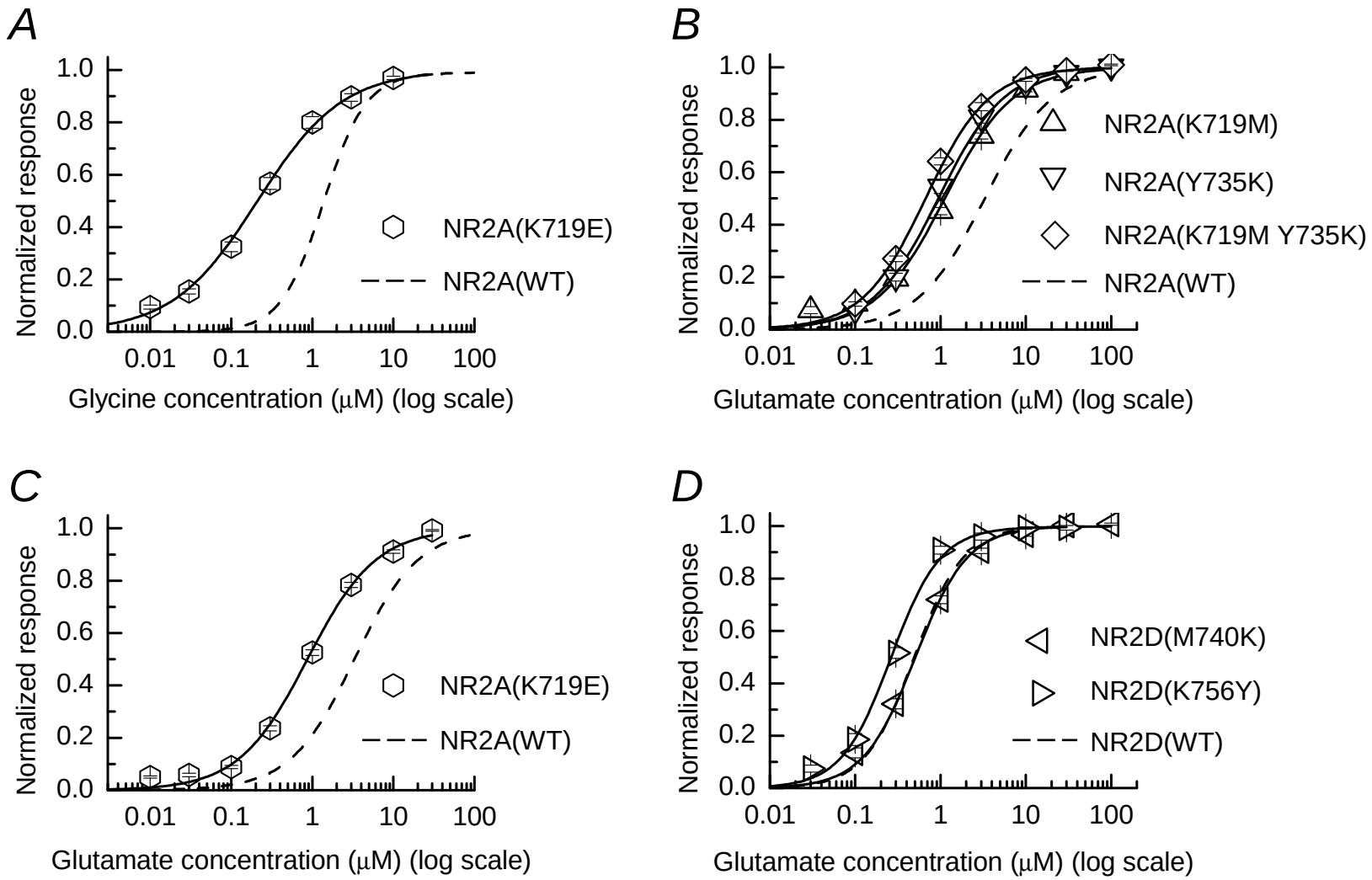

Supplemental Figure 5. Additional concentration-response curves for glycine and glutamate for mutations at Lys719 (NR2A) and Met740 and Lys756 (NR2D). *A*, mean glycine concentration-response curves for NR1/NR2A(K719E) NMDARs. This mutation also resulted in a shift to the left in glycine potency EC_{50} = 210 ± 10 nM, n_H = 0.83 ± 0.02, I_{max} = 3.0 ± 0.4 μM; *n* = 28). *B*, mean glutamate concentration-response curves for the NR2A(K719M), NR2A(Y735K) and NR2A(K719M Y735K) mutations. Small leftward shifts in each of these concentration-response curves were observed when compared to NR2A(WT)-containing NMDARs. The mean EC_{50} values, Hill slopes and maximal currents for these mutations were 1.11 ± 0.08 μM, 1.09 ± 0.06, 5.0 ± 0.3 μA (*n* = 14; NR2A(K719M)), 0.95 ± 0.05 μM, 1.13 ± 0.04, 1.9 ± 0.1 μA (*n* = 12; NR2A(Y735K)) and 0.67 ± 0.02 μM, 1.17 ± 0.02, 5.0 ± 0.4 μA (n = 12; NR2A(K719M Y735K). *C*, mean glutamate concentration-response curve for the NR2A(K719E) mutation. A small shift in glutamate potency was observed with a mean EC_{50} of 867 ± 110 nM, n_H = 1.02 ± 0.09, I_{max} = 4.7 ± 0.3 μA. *D*, mean glutamate concentration-response curves for the NR2D(M740K) and NR2D(K756Y) mutations. The mean EC_{50} values, Hill slopes and maximal currents for these mutations were 506 ± 66 nM, 1.23 ± 0.06, 0.35 ± 0.15 μA (*n* = 20; NR2D(M740K)) and 263 ± 11 nM, 1.49 ± 0.08, 0.2 ± 0.03 μA (*n* = 7; NR2D(K756Y)).